EUROPHYSICS LETTERS

21 January 1992

Europhys. Lett., **17** (4), pp. 321-326 (1992)

published in December 1991

Amplification of Thermal Noise via Convective Instability in Binary-Fluid Mixtures.

W. SCHÖPF and I. REHBERG

Physikalisches Institut der Universität Bayreuth - W-8580 Bayreuth, Germany

(received 10 June 1991; accepted in final form 24 October 1991)

PACS. 47.20 – Hydrodynamic stability and instability.
PACS. 47.25 – Turbulent flows, convection, and heat transfer.
PACS. 05.40 – Fluctuation phenomena, random processes, and Brownian motion.

Abstract. – In the convectively unstable regime of a binary-fluid mixture in a quasi–one-dimensional ramped convection channel an erratic spatio-temporal behaviour of very small amplitudes is observed. These patterns are interpreted as the amplification of intrinsic noise. Their measured temporal correlation functions are compared with the theoretical ones obtained from a Ginzburg-Landau equation containing a noise term. The measured intensity confirms the assumption that the fluctuations are due to thermal noise.

The influence of thermal noise on hydrodynamic instabilities, a problem of fundamental interest, has already been considered theoretically about 20 years ago [1, 2]. One of the predictions, a critical divergence of the fluctuation intensity similar to phase transitions in equilibrium thermodynamics, was considered as being too small to be observed directly ([1]). Thus some kind of amplification is necessary for an experimental observation. One method uses the exponential growth of fluctuations beyond threshold and has been applied in the case of stationary thermal convection [4]. Here we present measurements for travelling wave (TW) convection in a water-ethanol mixture [5-13], where the system offers an *intrinsic* amplification effect, namely the so-called convective instability [14].

The convective instability can be explained by using a linearized one-dimensional Ginzburg-Landau equation [15]

$$\tau_0(\partial_t + s\partial_x) A = \varepsilon A + \xi_0^2(1 + ic_1)\,\partial_x^2 A\,, \tag{1}$$

which describes the slow modulations of a small-amplitude TW near threshold. x is the horizontal dimension perpendicular to the rolls and $\varepsilon = (\Delta T - \Delta T_c)/\Delta T_c$ measures the distance from the critical temperature difference ΔT_c where convection sets in. For the case where side wall effects are negligible the coefficients have all been calculated from the underlying fluid equations [12, 13]. A linear stability analysis of eq. (1) for an infinite system shows that the trivial solution $A = 0$ is stable for $\varepsilon < 0$, convectively unstable for $0 < \varepsilon < \varepsilon_t$ and absolutely unstable for $\varepsilon > \varepsilon_t$ with $\varepsilon_t = (s\tau_0/2\xi_0)^2/(1 + c_1^2)$ [14]. In the convectively

([1]) In nematic liquid crystals a direct observation is possible, see ref. [3].

unstable situation a small local disturbance will increase in time, but is carried away by the group velocity s sufficiently fast to decay locally. Upon reaching the absolute instability point any small disturbance will increase locally—convection necessarily starts in the whole system.

In a finite system one usually cannot reach ε_t because the reflection of the TW from the sidewalls leads to an instability at some $\varepsilon_s < \varepsilon_t$. For not too small reflection coefficient r one finds $\varepsilon_s = -s\tau_0 \ln(r)/l$ (diffusion and dispersion effects, which will decrease ε_s, are neglected; l is the length of the cell) [10]. For conventional experimental situations ($l = 20$, $r = 0.4$) and the separation ratio $\Psi = -0.13$ one finds $\varepsilon_s \approx 0.01$ (while $\varepsilon_t \approx 0.1$) [12], and in an annulus [8] $\varepsilon_s = 0$. In our experiment we measure $\varepsilon_s = 0.06$, which is obtained by a special shape of the convection cell leading to a very small reflection coefficient. Thus we can work at relatively large ε without becoming absolutely unstable, and here the amplification of disturbances enables us to observe very small convection amplitudes.

In order to prevent three-dimensional effects, we use a thin convection channel which is cut out of a copper plate of thickness 1.5 mm [16, fig. 1]. Its homogeneous part has a height of $d = 3$ mm and is 18 mm long (x-direction). Adjacent to this central part parabolic ramps decrease the height of the channel from 3 mm to 1 mm over a length of 26 mm. These subcritical ramps decrease the amplitude of the waves travelling into this ramp leading to $r \approx 0.005$. The bottom of the cell is heated electrically and the top is kept at a constant temperature by a water circuit. The applied temperature difference ΔT is stable within ± 0.001 K. Our working fluid is a mixture of 16.98 wt.% of ethanol in water at a mean temperature of about 30 °C (Lewis number $L = 0.009$, Prandtl number $P = 10$, $\Psi = -0.13$) [17]. We measure the lateral temperature fluctuations using this shadowgraph technique by illuminating the cell from the side and taking the average of the light intensity over the vertical dimension. The light intensity modulation is then proportional to $|A|$.

In binary-fluid mixtures, one usually deals with a backward Hopf bifurcation [5, 11, 13]. This leads to the hysteresis shown in fig. 1. Here the amplitude of the convection is plotted as a function of ΔT. With increasing ΔT, stability is lost with respect to overturning convection at $\Delta T = 10.61$ K ($\varepsilon = 0.058$), and by cooling down the convection vanishes at the saddle node at $\Delta T = 9.61$ K ($\varepsilon = -0.042$). The important feature is the fact that this convection onset is well above the convective instability point $\Delta T = 10.03$ K ($\varepsilon = 0$, small arrow in fig. 1), which has been measured by determining the growth rate of a small heat pulse [18, 19]. (The branch inside the bifurcation diagram refers to stable confined states, which will be discussed in a further publication [19].)

To demonstrate the nature of the convective instability, fig. 2 shows a time series of the convection amplitude after a heat pulse has been applied to the system at $\varepsilon = 0.028$. To this purpose we put an electrical resistance on the outer glass of the cell at $x = 6.5d$, well inside

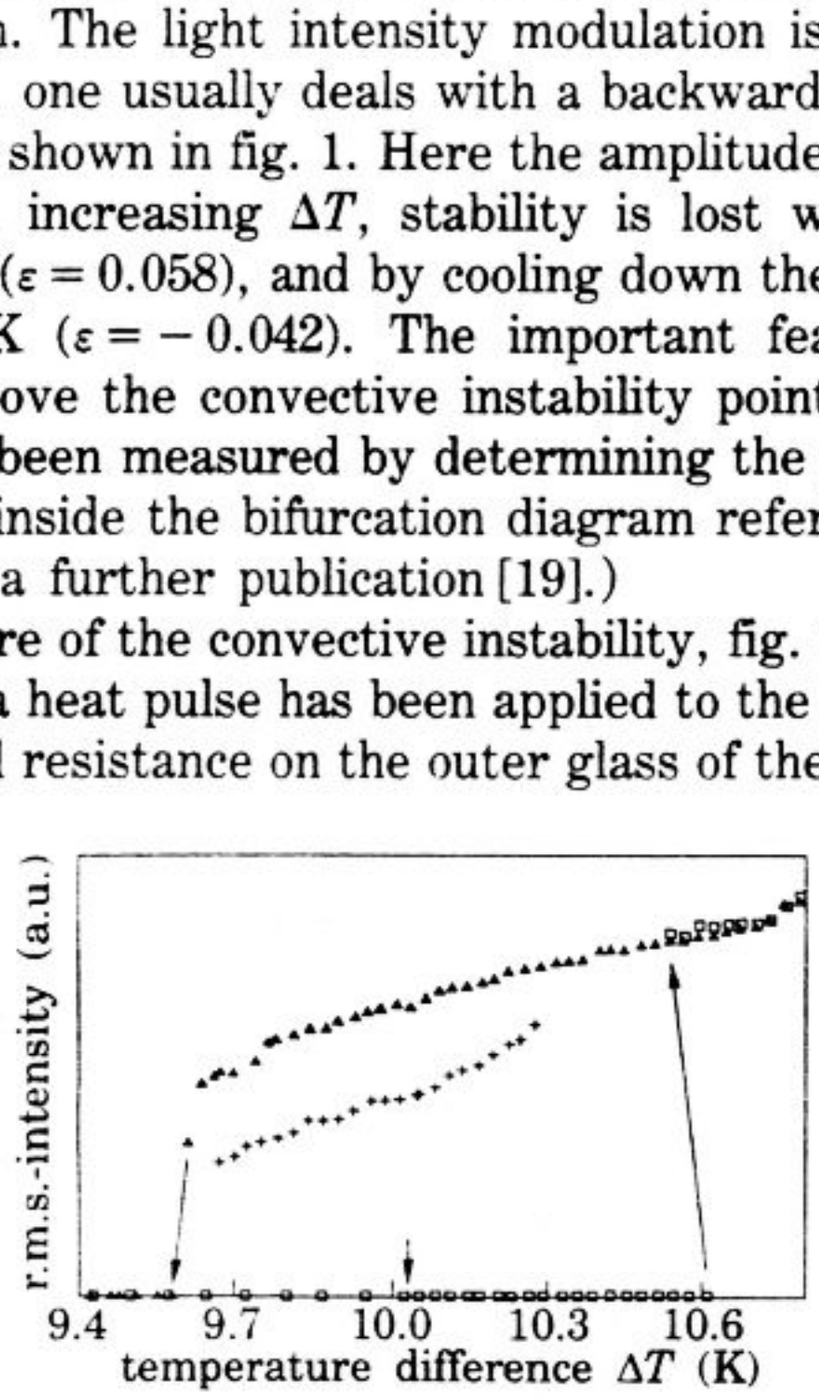

Fig. 1. – Bifurcation diagram. Squares correspond to increasing ΔT, triangles to decreasing ΔT and crosses to stable confined states. The convective instability point $\varepsilon = 0$ ($\Delta T = 10.03$ K) is indicated by the small arrow.

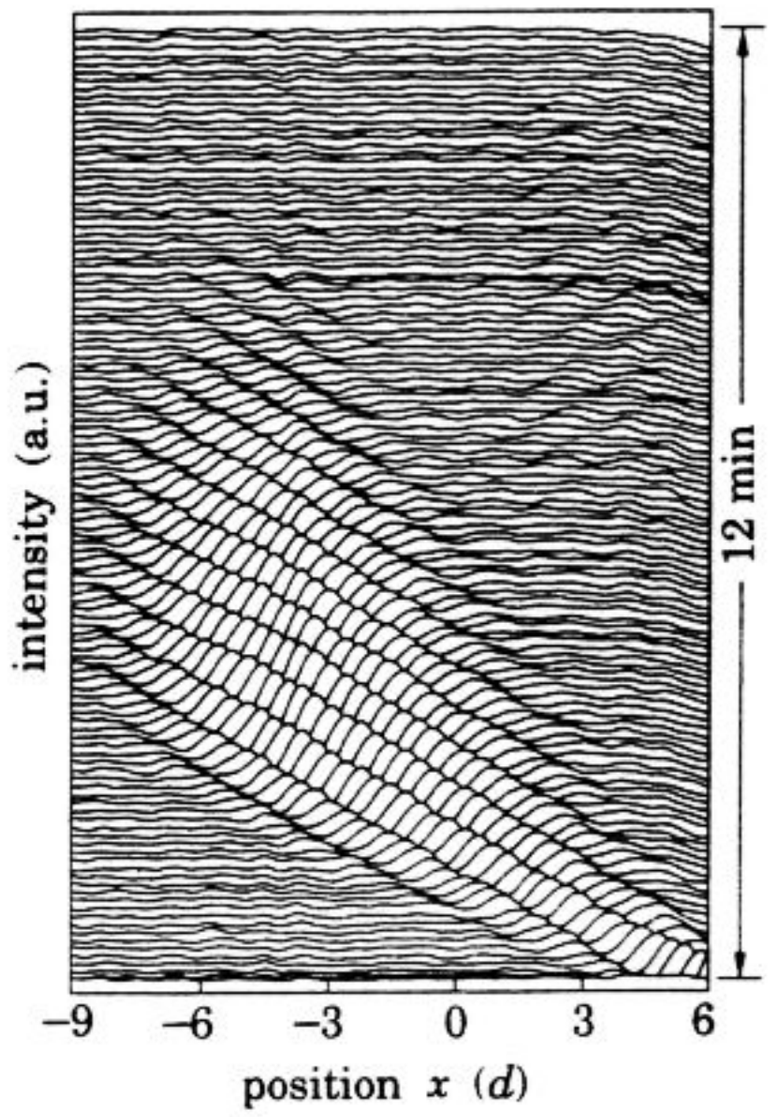

Fig. 2. – Spatio-temporal response to a heat pulse ($\varepsilon = 0.028$). $x = 0$ is the middle of the cell. The homogeneous region extends for $|x| < 3d$.

one of the ramps. The increase of the amplitude due to the unstable situation and the broadening of the pulse due to dispersion can be seen clearly. The spatial decrease of the amplitude due to the ramp at $x < -3d$ and the small reflection coefficient r are also demonstrated. With similar pulse techniques we measured $r = 0.005$ and the position where the TW are reflected [19].

The new feature presented here occurs in the range between the convective and the absolute instability point where we observe irregular spatio-temporal behaviour in the form of TW. They are of extremely small amplitude (between 0.01% and 1% of the fully developed convection on the upper branch of fig. 1) and consist of waves which increase in amplitude due to the convective instability while travelling through the cell [16, fig. 3]. Thus the amplitude of leftward TW is larger in the left part of the cell, but hardly detectable in the right part, where the rightward TW dominates. While the amplitude and the spatio-temporal coherence of those structures increase with increasing ε, the frequency of the TW stays nearly constant at the Hopf frequency (28.5 s/period). This state is not a transient, in our longest run it persisted without qualitative changes for about ten days. Figure 3 shows the envelope of the appropriately filtered light intensity signal of such a state for $\varepsilon = 0.051$ at $x = \pm 3d$ where the amplitude is amplified the most by the convective nature of the instability. The upper (lower) curve has been measured in the left (right) part of the cell, where the intensity is basically determined by the leftward (rightward) TW, while the rightward (leftward) TW has a hardly measurable, but finite amplitude. We found no hint of a regularity for the occurrence of the bursts, although they seem to have some typical lifetime. Also there is no correlation between the bursts on the left- and right-hand side, which indicates that this state is different from the «blinking state» observed in former experiments [7]. Moreover, this lack of correlation indicates that these structures are not driven by external fluctuations. The possibility that this state is due to a chaotic attractor seems unlikely since we are talking about very small amplitudes, where only linear interactions are important. The behaviour illustrated in fig. 3 is qualitatively the same in the whole convectively unstable regime.

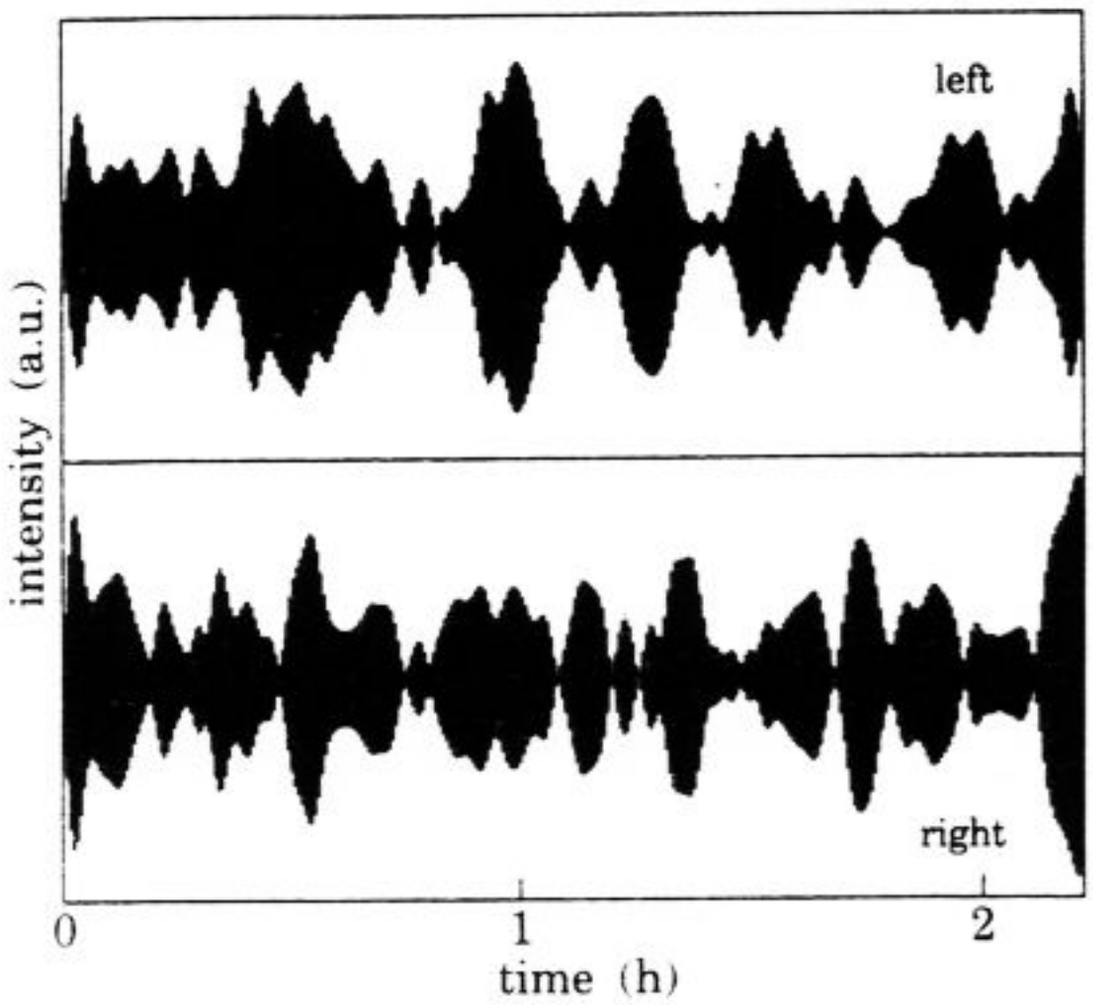

Fig. 3.

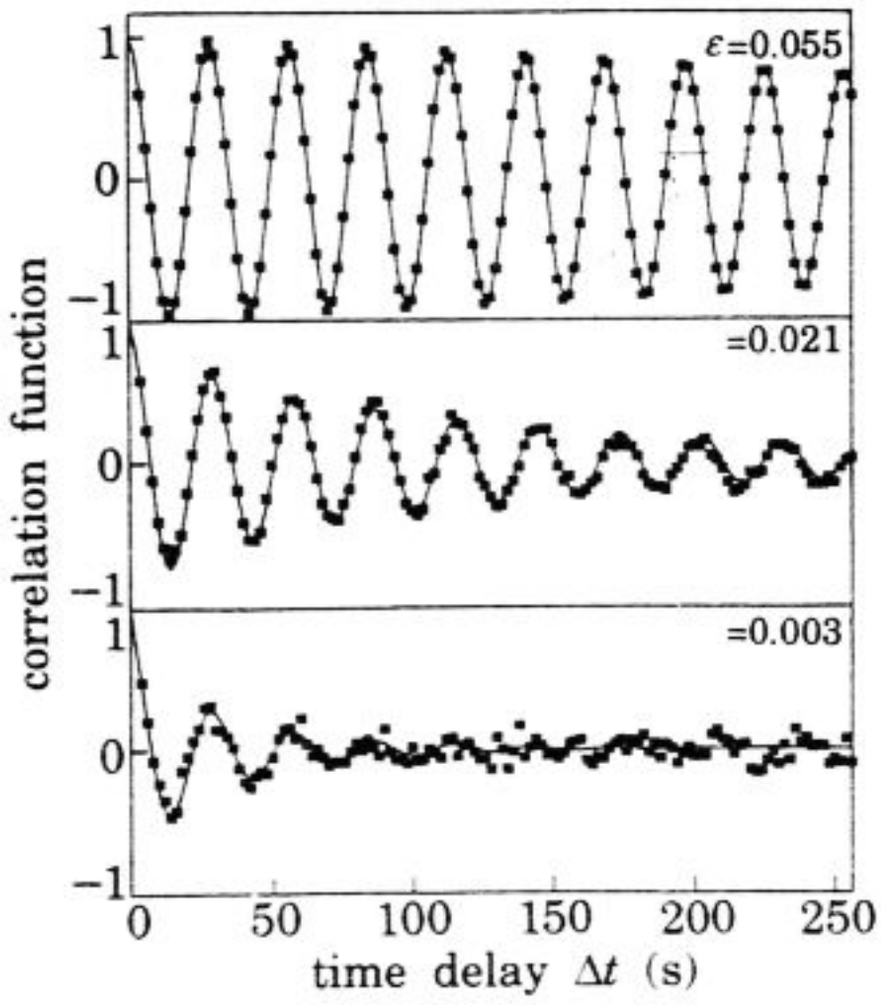

Fig. 4.

Fig. 3. – Light intensity measured at $x = -3d$ (left) and $x = +3d$ (right) for $\varepsilon = 0.051$ ($\Delta T = 10.54$ K).

Fig. 4. – Temporal correlation function of the small amplitude convection for three different ε. The squares represent the experimental data and the lines are fits according to eq. (3).

For a quantitative analysis of these structures we measure the time correlation function $C(\Delta t)$ at $x = 3d$. To get a theoretical expression for $C(\Delta t)$, we consider a linearized equation (we are looking at very small amplitudes) with a noise term:

$$\tau_0(\partial_t + s\partial_x) A = -\alpha A + \xi_0^2 \partial_x^2 A + \sqrt{Q} F(x, t)\,, \tag{2}$$

where $\sqrt{Q}F(x, t)$ represents external or internal noise and its space-time correlation is given by $\langle F^*(x, t) F(x + \Delta x, t + \Delta t)\rangle = \delta(\Delta x)\,\delta(\Delta t)$ [2]. For simplicity all coefficients in eq. (2) are taken real. Using Fourier transform techniques one obtains for the temporal correlation [3, 19]

$$C(\Delta t) := \langle A^*(t) A(t + \Delta t)\rangle \cos(\omega \Delta t) = Q/(8\tau_0 \xi_0 \alpha^{1/2}) \cos(\omega \Delta t) \cdot$$

$$\cdot \left\{ \exp\left[\frac{\Delta t}{t_1}\right] \operatorname{erfc}\left(\sqrt{\frac{\Delta t}{t_0}} + \frac{1}{2}\sqrt{\frac{\Delta t \cdot t_0}{t_1^2}} \right) + \exp\left[-\frac{\Delta t}{t_1}\right] \operatorname{erfc}\left(\sqrt{\frac{\Delta t}{t_0}} - \frac{1}{2}\sqrt{\frac{\Delta t \cdot t_0}{t_1^2}} \right) \right\}. \tag{3}$$

We introduced the times $t_0 = \tau_0/\alpha$ and $t_1 = \xi_0/(s\alpha^{1/2})$, which measure the decay of a spatially uniform and a spatially modulated state, respectively. The term $\cos(\omega\,\Delta t)$ must be included to represent the rapid oscillation due to the Hopf frequency.

Equation (2) describes a transition, where the intensity $Q/(8\tau_0 \xi_0 \alpha^{1/2})$ and the times t_0 and t_1 diverge at $\alpha = 0$. In our measurements this is the case at ΔT_s, so we have to set $\alpha = (\Delta T_s - \Delta T)/\Delta T_s$ in order to model our experimental situation. This is necessary to deal with the absolute instability, which forces the nonlinear convection to occur at $\alpha = 0$ rather than at $\varepsilon = 0$. The numerical values of the coefficients τ_0, s and ξ_0 are expected to be only slightly shifted compared to the ones in eq. (1). One sees that by including spatial degrees of freedom one gets a nonexponential decay of the correlation function, even in the case of a stationary bifurcation ($s = 0$) ([2]).

([2]) By mistake, in [2, eq. (5.46)] an exponential decay was presented (R. Graham, private communication).

Figure 4 shows the measured correlation function scaled to 1 at $\Delta t = 0$ for three different ε, together with a fit according to eq. (3). For large $\varepsilon(0.055)$ this yields a nearly perfect cosine with the underlying Hopf frequency, while for decreasing ε this function becomes more noisy and decays faster in time. Figure 5 shows the results of the fits as a function of ΔT. The values obtained for t_0 and t_1 are plotted together with a fit to the expected power laws, namely α^{-1} and $\alpha^{-1/2}$. This yields $\tau_0 \approx 24$ s and $\xi_0/s \approx 11$ s, which are in reasonable agreement with the theoretical values for an infinite system when times are rescaled with the measured thermal diffusion time of our system [12]. For small ε the uncertainties for t_0 and t_1 become large. This is illustrated in the lower part of fig. 4, where nevertheless the frequency and the amplitude can be extracted with good accuracy. The frequency ω above the convective instability point $\varepsilon = 0$ (indicated by the arrows in fig. 5) stays nearly constant except for a slight increase with ε. Below this point the experimental data are harder to analyse, leading to a larger scatter in ω.

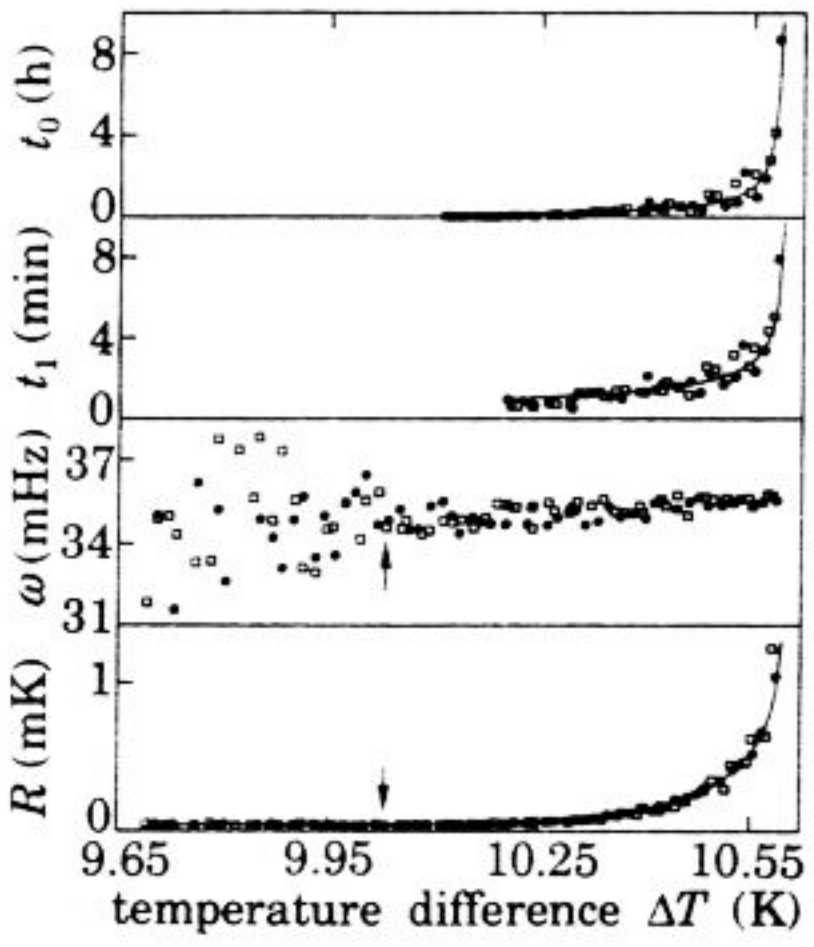

Fig. 5. – Parameters extracted from fits like those in fig. 4 for increasing ΔT (squares) and for decreasing ΔT (circles). The lines are fits to the expected ε-laws.

In the lower part of fig. 5, we fit

$$R = \sqrt{(\langle A^* A \rangle)} = \sqrt{\bar{Q}/\alpha^{1/2}} \exp\left[\frac{x_m}{\tau_0 s}\varepsilon\right]$$

(solid line) to the measured amplitude, thus taking into account the amplification via the convective instability by a factor of $\exp[(x_m/\tau_0 s)\varepsilon]$. This has to be done because eq. (3) describes the answer of the system to the fluctuations present at the chosen $x = 3d$, which are already amplifications of the underlying noise. x_m characterizes the mean distance between the origin of the disturbances (which of course are not expected to have a well-defined source) and the measurement point. The measured r.m.s.-amplitude R is proportional to the lateral temperature variation in the liquid. Our smallest signal corresponds to less than 10^{-4} K (at $\varepsilon = -0.03$). For $\bar{Q}^{1/2}$ we get from this procedure about $2 \cdot 10^{-6}$ K, while the thermodynamic fluctuations for a stationary bifurcation in an infinite system with free boundary conditions should lead to $\bar{Q}^{1/2} \approx 5 \cdot 10^{-6}$ K [2]. These values agree reasonably well taking into account an experimental error of a factor of two and the fact that not all of the fluid parameters are known accurately. Analog to ref. [2] we have calculated the fluctuations

for the Hopf bifurcation (still in an infinite system with free boundaries). The results does not change drastically and we get $\bar{Q}^{1/2} \approx 3 \cdot 10^{-6}$ K [19].

In summary the amplification via the convective instability is a good instrument to measure very small temperature fluctuations. The resulting spatio-temporal behaviour is adequately described by the above-given ansatz leading to two different correlation times with different critical exponents. The measured fluctuation intensity seems to be driven by thermal fluctuations.

* * *

We thank M. LÜCKE and L. KRAMER for useful suggestions. The experiment was supported by Volkswagen-Stiftung.

REFERENCES

[1] ZAITSEV V. M. and SHLIOMIS M. I., *Sov. Phys. JETP*, **32** (1971) 866.
[2] GRAHAM R., *Phys. Rev. A*, **10** (1974) 1762.
[3] REHBERG I., RASENAT S., DE LA TORRE JUÁREZ M., SCHÖPF W., HÖRNER F., AHLERS G. and BRAND H. R., *Phys. Rev. Lett.*, **67** (1991) 596.
[4] AHLERS G., CROSS M. C., HOHENBERG P. C. and SAFRAN S., *J. Fluid. Mech.*, **110** (1981) 297; MEYER C. W., AHLERS G. and CANNEL D. S., *Phys. Rev. A*, in print.
[5] For a review of the older literature, see PLATTEN J. K. and LEGROS L. C., *Convection in Liquids* (Springer, New York, N.Y.) 1983.
[6] See, *e.g.*, KOLODNER P., PASSNER A., SURKO C. M. and WALDEN R. W., *Phys. Rev. Lett.*, **56** (1986) 2621; SULLIVAN T. and AHLERS G., *Phys. Rev. Lett.*, **61** (1988) 78; FINEBERG J., MOSES E. and STEINBERG V., *Phys. Rev. Lett.*, **61** (1988) 842.
[7] MOSES E., FINEBERG J. and STEINBERG V., *Phys. Rev. A*, **35** (1987) 2757.
[8] KOLODNER P., BENSIMON D. and SURKO C. M., *Phys. Rev. Lett.*, **60** (1988) 1723.
[9] See, *e.g.*, BRAND H. R., HOHENBERG P. C. and STEINBERG V., *Phys. Rev. A*, **30** (1984) 2548; KNOBLOCH E. and MOORE D., *Phys. Rev. A*, **37** (1988) 860.
[10] CROSS M., *Phys. Rev. Lett.*, **57** (1986) 2935.
[11] LINZ S. J. and LÜCKE M., *Phys. Rev. A*, **36** (1987) 3505.
[12] CROSS M. and KIM K., *Phys. Rev. A*, **37** (1988) 3909.
[13] SCHÖPF W. and ZIMMERMANN W., *Europhys. Lett.*, **8** (1989) 41.
[14] DEISSLER R. J., *J. Stat. Phys.*, **40** (1985) 371; HUERRE P., in *Instabilities and Nonequilibrium Structures*, edited by E. TIRAPEGUI and D. VILLAROEL (Reidel, Dordrecht) 1987.
[15] NEWELL A. C., *Lect. Appl. Math.*, **15** (1974) 157; BRAND H. R., LOMDAHL P. S. and NEWELL A. C., *Physica D*, **23** (1986) 345.
[16] SCHÖPF W. and REHBERG I., in *Nonlinear Evolution of Spatio-Temporal Structures in Dissipative Continuous Systems*, edited by F. H. BUSSE and L. KRAMER (Plenum Press, New York, N.Y.) 1990.
[17] KOLODNER P., WILLIAMS H. and MOE C., *J. Chem. Phys.*, **88** (1988) 6512.
[18] KOLODNER P., SURKO C. M., PASSNER A. and WILLIAMS H. L., *Phys. Rev. A*, **36** (1987) 2499.
[19] SCHÖPF W., in preparation.